Biocatalysis and Biotransformation

ISSN: 1024-2422 (Print) 1029-2446 (Online) Journal homepage: https://tandfonline.com/loi/ibab20

Characterization of a recombinant β-xylosidase of GH43 family from *Bacteroides ovatus* strain ATCC 8483

Andong Zhou, Yanbo Hu, Jingjing Li, Weiyang Wang, Mengshan Zhang & Shuwen Guan

To cite this article: Andong Zhou, Yanbo Hu, Jingjing Li, Weiyang Wang, Mengshan Zhang & Shuwen Guan (2019): Characterization of a recombinant β-xylosidase of GH43 family from *Bacteroides ovatus* strain ATCC 8483, Biocatalysis and Biotransformation, DOI: 10.1080/10242422.2019.1631813

To link to this article: https://doi.org/10.1080/10242422.2019.1631813

BIOCATALYSIS AND BIOTRANSFORMATION
https://doi.org/10.1080/10242422.2019.1631813

Taylor & Francis
Taylor & Francis Group

RESEARCH ARTICLE

Characterization of a recombinant β-xylosidase of GH43 family from *Bacteroides ovatus* strain ATCC 8483

Andong Zhou[a#], Yanbo Hu[b#], Jingjing Li[c], Weiyang Wang[b], Mengshan Zhang[b] and Shuwen Guan[a]

[a]School of Life Sciences, Jilin University, Changchun, China; [b]School of Life Sciences, Northeast Normal University, Changchun, P. R. China; [c]Beijing Institute of Metrology, Beijing, China

ABSTRACT

A novel β-1,4-xylosidase was identified from the genome of *Bacteroides ovatus* strain ATCC 8483 and overexpressed in *Escherichia coli* BL21 (DE3) cells. The molecular weight of recombinant enzyme named BoXyl43A was calculated to be 37.1 kDa. Using *p*-nitrophenyl-β-D-xylopyranoside (*p*NPβXyl) as substrate, BoXyl43A was most active at pH 7.0 and 35 °C. The enzyme could be activated by Mg^{2+} and Mn^{2+}. The K_m and V_{max} of BoXyl43A against *p*NPβXyl were 1.71 ± 0.21 mM, 7.41 ± 0.81 μmol/min/mg, respectively. BoXyl43A hydrolyzed xylooligosaccharide to produce D-xylose as main product, indicating that BoXyl43A acted as an exo-β-1,4-xylosidase. The mixture of BoXyl43A and PoAbf62A (α-L-arabinofuranosidase) exhibited significant synergistic effects on the degradation of arabinoxylan. Therefore, BoXyl43A would be a useful tool to degrade hemicellulose.

ARTICLE HISTORY
Received 29 August 2018
Accepted 3 June 2019

KEYWORDS
Bacteroides ovatus; β-1,4-xylosidase; GH family 43

Introduction

Lignocellulosic biomass is the most abundant renewable resource in the world; it shows great potential in production of biofuels and valuable chemicals by using lignocellulose (Gírio et al. 2010). Lignocellulose is mainly composed of cellulose, hemicellulose and lignin (Isikgor and Becer 2015). β-1,4-D-xylan makes up over 50% of the total content of hemicellulose. Xylan backbones are substituted at O-2/O-3 sites by different substituents, including α-L-arabinofuranose, glucuronic acid and/or 4-O-methyl-glucuronic acid, ferulic acid and acetyl groups (Scheller and Ulvskov 2010; Juturu and Wu 2012; Cintra et al. 2017).

Due to structural diversity, degradation of hemicellulose requires many different hemicellulases synergistically acting on the backbone and branched chains of xylan (Saha 2003; Lagaert et al. 2014), including endoxylanase, β-xylosidase, α-L-arabinofuranosidase, α-glucuronidase and acetylxylan esterase (Cragg et al. 2015; Mendis and Simsek 2015). β-Xylosidases are important enzymes for hydrolyzing xylooligosaccharides and xylobiose to release xylose. They are used in many biotechnological processes. β-Xylosidases are classified into families GH1, 3, 5, 30, 39, 43, 51, 52, 54, 116 and 120 based on their amino acid sequence similarity (Knob et al. 2010). The enzymes of GH43 family mainly include β-xylosidase and α-L-arabinofuranosidase. Some enzymes of GH43 family have both β-xylosidase and α-L-arabinofuranosidase functions (Jordan et al. 2013), which enable them to hydrolyze a diverse range of fiber substrates (Khandeparker and Numan 2008; Carvalho et al. 2018). Identification and utilization of novel hemicellulolytic enzymes is of potential use for the structure analysis of hemicellulose and conversion of hemicellulosic biomass into biofuels.

Bacteroides ovatus is a common human gut bacterium capable of degrading and growing on several plant cell wall polysaccharides with complex structure. Genomic analysis indicated that *B. ovatus* possesses several unique polysaccharide utilization loci (PULs) that enable degradation of hemicellulosic polysaccharides (Martens et al. 2011; Zhang et al. 2014). In this manuscript, a novel β-xylosidase belonging to GH43 family was identified from *B. ovatus*.

Materials and methods

Strains and reagents

Bacteroides ovatus strain ATCC 8483 was purchased from China General Microbiological Culture Collection

CONTACT Mengshan Zhang zhangms253@nenu.edu.cn School of Life Sciences, Northeast Normal University, Changchun 130024, China
#These authors contributed equally to this work.

Supplemental data for this article can be accessed here.

Center. *E. coli* BL21 (DE3) and pET-28a (+) were used as host and expression vector, respectively (Novagen, Madison, WI, USA). *p*-Nitrophenyl-β-glucopyranoside (*p*NPβGlc), *p*NP-α-glucopyranoside (*p*NPαGlc), *p*NP-β-galactopyranoside (*p*NPβGal), *p*NP-α-galactopyranoside (*p*NPαGal), *p*NP-β-mannopyranoside (*p*NPβMan), *p*NP-α-mannopyranoside (*p*NPαMan), *p*NP-β-xylopyranoside (*p*NPβXyl), *p*NP-α-L-arabinofuranoside (*p*NPαAraf) were from Sigma (St. Louis, MO). Genomic DNA isolation, DNA purification, and plasmid isolation kits were from Tian gen Biotech (Beijing, China).

Cloning and expression of boxyl43a gene

Genomic DNA of *B. ovatus* was isolated using Tian gen genomic DNA isolation kit. The primers having restriction sites for *Eco*RI (5′ - CGGAATTCATGAAAAAAGAAA TGAGATACC-3′) and *Xho*I (5′- CCGCTCGAGTTACTA CGCTCCTCCATCTAT-3′) were used for gene *boxyl43a* amplification. PCR was performed using DreamTaq Green PCR Master Mix (Thermo Scientific) and the program was as follows: 95 °C for 5 min, 30 cycles of 95 °C for 30 s, 63 °C for 45 s, 72 °C for 1 min, and final extension at 72 °C for 10 min. The PCR product and pET-28a (+) were digested with *Eco*RI and *Xho*I, respectively. Then *boxyl43a* gene was ligated with pET-28a (+) to generate the recombinant plasmid pET28a-*boxyl43a*. Obtained recombinant amplicon was analyzed by *Comate Bioscience Co. Ltd.* (Changchun, China) with T7 and T7-ter as sequencing primers. For BoXyl43A expression, *E. coli* BL21 (DE3) cells harboring pET28a-*boxyl43a* were grown in 200 mL of LB culture with 50 μg/mL kanamycin at 37 °C, 160 rpm. After the $OD_{600\,nm}$ of bacteria reached 0.6, the culture was induced with 0.5 mM IPTG and grown overnight at 25 °C for expression of BoXyl43A.

Purification of recombinant BoXyl43A

Recombinant cells were harvested by centrifugation at 8000 rpm for 10 min and suspended in 20 mL of lysis buffer (20 mM phosphate buffer, pH 7.0, 0.1 M NaCl) and then disrupted by sonication on ice (3 s pulses with 6 s interval for 10 min). Cell debris was removed by centrifugation at 4 °C and 13,000 rpm for 45 min, and crude protein was obtained in supernatant. Recombinant BoXyl43A carrying His-tag was loaded onto Ni^{2+} affinity column (GE healthcare). The 2 mL Ni^{2+} column was pre-equilibrated with the binding buffer, washed with 20 mL washing buffer (20 mM phosphate buffer, pH 7.0, 0.1 M NaCl, 20 mM imidazole) and then eluted with 20 mL eluting buffer (20 mM phosphate buffer, pH 7.0, 0.1 M NaCl, 250 mM imidazole). The active fractions were pooled and dialyzed against 20 mM phosphate buffer, pH 7.0. The purified protein was analyzed by sodium dodecyl sulfate-polyacrylamide gel electrophoresis (SDS-PAGE) on 10% separating gel. Protein concentrations were determined by the method of Bradford using bovine serum albumin (BSA) as a standard.

Characterization of recombinant BoXyl43A

Assay of the specific activity of BoXyl43A was carried out in 200 μL of 20 mM phosphate buffer (pH 7.0) containing 5 mM substrate and 2 μg recombinant BoXyl43A. After incubating at 30 °C for 5 min, the reaction was stopped by adding 50 μL Na_2CO_3 (0.5 M), and the released *p*-nitrophenol was measured at 405 nm by BioTek ELx808 microplate reader (Winooski, VT, USA). The reaction mixture without enzyme was used as the control. At assay conditions of pH 7.0, 30 °C, the amount of enzyme releasing 1 μmol/min of *p*-nitrophenyl was defined as one unit (U).

Effect of pH on BoXyl43A activity was determined at pH 2.0-11.0 using *p*NPβXyl (5 mM) as substrate. The pH stability was determined under standard assay conditions after incubation of the purified BoXyl43A for 24 h at 4 °C in the buffers without substrate. The effect of temperature on BoXyl43A activity was investigated by measuring the BoXyl43A activity at temperatures ranging from 30 °C to 50 °C. Thermostability was determined by incubating the enzyme at the temperatures from 30 °C to 50 °C for 1 h 30 min. Residual activities were measured as described before. The initial activity without incubation was set as 100%.

The effects of metal ions and chemicals on the activity of BoXyl43A were determined by incubating purified enzyme with each metal ion or chemical (5 or 50 mM) for 24 h at 4 °C. The reaction mixture without enzyme was used as the control. The activity of BoXyl43 assayed in the absence of metal ions or chemical was taken as 100%, and then the residual activity was determined using *p*NPβXyl as substrate.

Determination of kinetic parameters

To determine the kinetic parameters for *p*NPβXyl, the buffer used was identical to that stated above and five substrate concentrations ranging from 0.2 mM to 1 mM were used. Reactions were initiated with 20 μL BoXyl43A (0.1 mg/mL) and production of *p*NP was monitored at 405 nm every 15 s. The time courses were linear for the first 2 min, and the rate was

determined from a tangent to a curve measured. The K_m and V_{max} values were calculated from GraphPad Prism V5.

Substrate specificity

Substrate specificity was determined using various *p*NP-glycosides as substrates, and the reaction was carried out in 200 μL of 20 mM phosphate buffer (pH 7.0) containing 5 mM substrates and 2 μg BoXyl43A. The reaction mixture without enzyme was used as the control. Hydrolytic activity towards polysaccharides was determined at 37 °C in phosphate buffer (pH 7.0), with 0.5% (wt/vol) polysaccharides as substrates and 5 μg BoXyl43A. After incubation for 1 h or 12 h, liberated reducing sugars were measured by the method of Somogyi (1952). To determine hydrolyzates of different polysaccharides, a reaction mixture containing 50 μL of a 4 mg/ml substrate solution, 140 μL of 20 mM phosphate buffer (pH 7.0), and 10 μL of BoXyl43A (100 μg/mL) was incubated for 12 h at 37 °C. The enzymatic products were analyzed by using high-performance anion-exchange chromatography (HPAEC) using a CarboPac PA-200 analytical column (3 × 250 mm) as described in our previous work (Hu et al. 2018).

Synergistic action of BoXyl43A with α-L-arabinofuranosidase in degradation of arabinoxylan

Hydrolysis of arabinoxylan was determined by incubating arabinoxylan (10 mg/mL) with α-L-arabinofuranosidase (PoAbf62A, final concentration 10 μg/mL), or 10 μg/mL BoXyl43A, or both. In reactions with both enzymes, arabinoxylan was incubated with α-L-arabinofuranosidase for 12 h at 37 °C, pH 4.5, and then BoXyl43A was added to the reaction for 12 h after adjusting in buffer to pH 7.0. To identify the hydrolysis products, reducing sugars released from the reaction were analyzed by the HPAEC method mentioned above.

Nucleotide sequence accession number

The sequence of BoXyl43A gene from *B. ovatus* strain ATCC 8483 was deposited in Genbank under accession numbers MK726378.

Results and discussion

Cloning, expression and purification of recombinant BoXyl43A

BoXyl43A was obtained from genome sequence of *B. ovatus* strain ATCC 8483 and contains 324 amino acids, and the molecular weight of BoXyl43A was calculated to be 37.1 kDa (https://web.expasy.org/protparam/). According to the amino acid sequence of BoXyl43A from 15 to 319, it probably belongs to the GH43 family (CAZy database: http://www.cazy.org/CAZY). Amino acids of N-terminal from 1 to 12 were predicted to be a signal peptide. According to nucleic acid sequence, the gene was cloned into *p*ET-28a(+) (*Eco*RI/*Xho*I), and *E.coli* BL21 (DE3) was chosen as host cell of BoXyl43A. The nucleic acid sequence of BoXyl43A is shown in Supplementary Figure S1. BoXyl43A was expressed as soluble protein in *E.coli* BL21 (DE3). The enzyme activity was determined by measuring the increase in absorbance of the reaction mixture at 405 nm using *p*NPβXyl as the substrate. As shown in Table 1, BoXyl43A was highly expressed and the concentration of total protein was 390 mg/L culture. BoXyl43A was purified by Ni^{2+} affinity column with a yield of 45.3%, and a specific activity of 4.9 U/mg. The purified BoXyl43A was analyzed by SDS-PAGE gel and almost no other protein bands were observed on the gel (Figure 1).

Biochemical characterization of recombinant BoXyl43A

The enzymatic activity of BoXyl43A was examined over a pH range from 2.0 to 11.0 with *p*NPβXyl as the substrate. Our results showed that BoXyl43A exhibited the maximum activity at pH 7.5, and it was stable within the pH range from 6.0 to 7.0 (Figure 2). The effect of temperature on the enzyme activity was investigated at optimal pH, and BoXyl43A exhibited

Table 1. Summary of purification of recombinant BoXyl43A.

Purification step	Volume (ml)	Total protein (mg)[a]	Activity (U)[b]	Sp act (U/mg)	Purification (fold)	Yield (%)
Crude enzyme extract	15.0	78.0	210	2.70	1.00	100
Ni sepharose fast flow column	3.00	19.5	94.5	4.90	1.80	45.3

[a]Protein was quantified according to the Bradford Method using bovine serum albumin (BSA) as standard.
[b]The activity was reported as activity on *p*NPβXyl.

the maximum activity at 35 °C. The thermostability of BoXyl43A was investigated ranging from 30 to 50 °C at a constant pH of 7.0. As shown in Figure 3, approximately 80% of its activity remained after the treatment of 35 °C for 90 min. However, the activity significantly decreased above 40 °C. Therefore, pH 7.0 and temperature of 35 °C were chose as optimum conditions in degradation of hemicellulose .

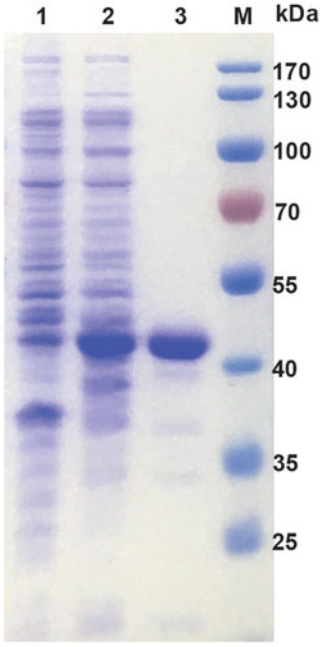

Figure 1. SDS-PAGE analysis of recombinant BoXyl43A on 10% resolving gel. Lane 1, culture lysate of *E. coli* BL21-pET28a-*boxyl43a* before IPTG induction; lane 2, supernatant of the culture lysate of *E. coli* BL21-pET28a-*boxyl43a* after IPTG induction; lane 3, BoXyl43A purified from Ni^{2+} sepharose fast-flow column which showed target band; M, molecular weight marker (PageRuler Prestained Protein Ladder, Genestar).

Regarding the effect of metal ions and chemicals on BoXyl43A, $Mg^{2+}$and Mn^{2+} at a concentration of 5 mM increased its activity more than 70% (Table 2). The results indicated that Mg^{2+} and Mn^{2+} might affect the activity of β-xylosidases, consistent with those results in the literature (Kim and Yoon 2010; Lee et al. 2013). Na^{+}, K^{+} and DTT did not affect the activity of BoXyl43A significantly, but the activity of BoXyl43A was strongly inhibited by 5 mM Ca^{2+}, Ba^{2+}, Hg^{2+}, Cu^{2+}, Fe^{3+}, SDS and DTT.

To get information regarding the active site residues of BoXyl43A, we compared the amino acid sequences to four β-xylosidases from GH 43 family, RS233BX (Genbank AFP23142.1), RUM630-BX (Genbank AFE48532.1), CoXyl (Genbank BAS02080.1) and BoXA (Genbank AAB08024) (Jordan et al. 2015; Jordan et al. 2016; Matsuzawa et al. 2017; Jordan et al. 2017), respectively. Knowing the residue numbers of the active site residues of RS223-BX from the X-ray structure (PDB ID 4MLG), we could do a linear alignment of the primary structures to find amino acid residues in the active-site pocket of the other β-xylosidases. The multiple amino acid sequence alignment indicated BoXyl43A had 75, 59, 54, and 80% identity to RS233BX, RUM630-BX, CoXyl and BoXA, respectively. It is obvious that the active-site residues D16 (catalytic base), D137 (transition-state stabilizer) and E224 (catalytic acid) are conserved in all of these sequences (Supplementary Figure S2), and amino acid residues D86 and H275 are related to combination of divalent metal. Besides, there were 17 other amino acid residues in the active site pocket, most of which are conserved, except the sites of 86, 110, 136 and 244. And the amino acid residues in the active-site pocket of

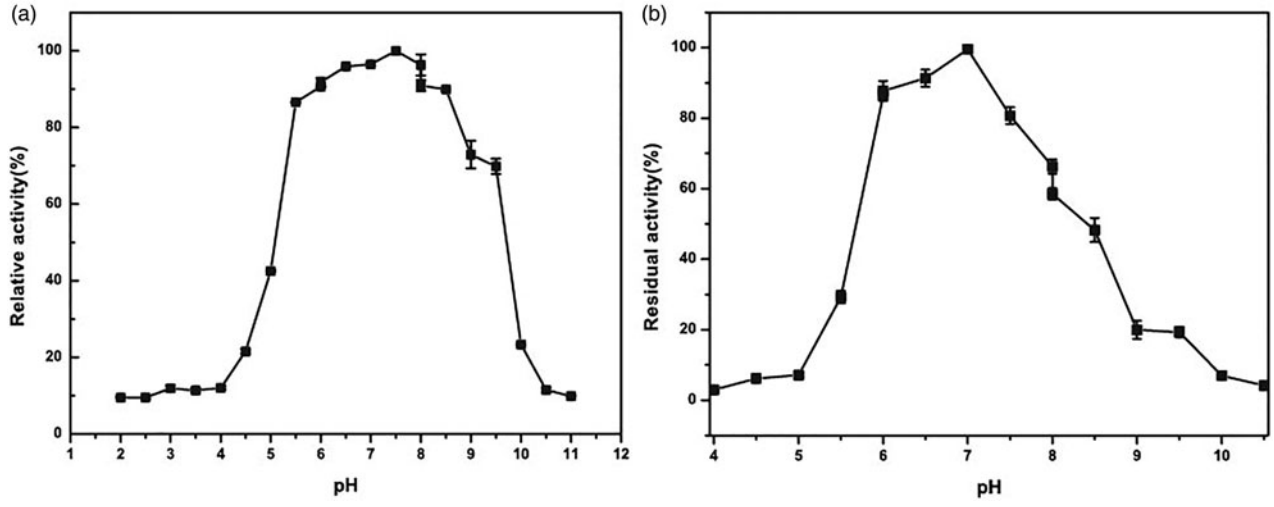

Figure 2. Effect of pH on activity (a) and stability (b) of BoXyl43A using *p*NPβXyl as substrate. The activity of BoXyl43A without pre-incubating was defined as 100%. Results are presented as means ± standard deviations (n = 3).

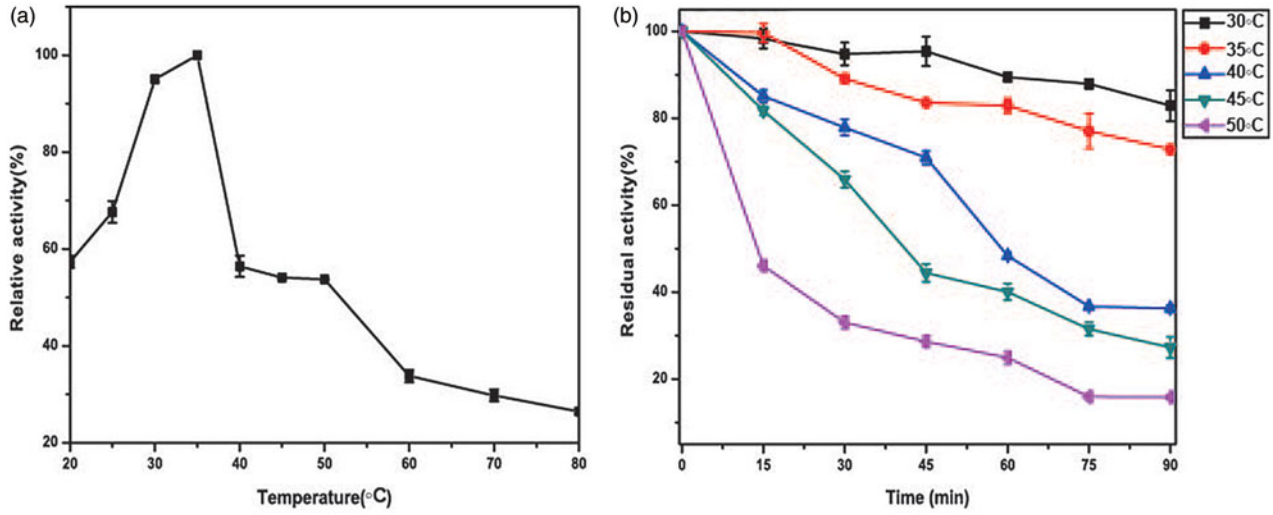

Figure 3. Effect of temperature on activity (a) and stability (b) of BoXyl43A using *p*NPβXyl as substrate. The optimal temperature was determined at different temperatures ranging from 20 to 80 °C. The maximum activity obtained was defined as 100% activity. Thermal stability was determined by incubating the enzyme for 1 h 30 min at different temperatures. The activity of the enzyme before incubation was defined as 100%. Results are presented as means ± standard deviations (n = 3).

Table 2. Effects of metal ions and chemical agents on the activity of BoXyl43A.

	Relative activity	
Metal ions or reagents	5 mM	50 mM
EDTA	27.7 ± 2.4	2.70 ± 0.0
DTT	98.9 ± 2.4	79.8 ± 1.2
NaCl	88.9 ± 1.6	76.0 ± 2.6
SDS	2.80 ± 0.1	2.50 ± 0.0
$MgCl_2$	178 ± 3.2	198 ± 0.6
KCl	92.6 ± 0.7	85.6 ± 4.2
$CaCl_2$	22.5 ± 0.9	—
$BaCl_2$	17.5 ± 1.0	—
$HgCl_2$	4.80 ± 0.5	—
$CuCl_2$	9.30 ± 0.1	—
$MnCl_2$	216 ± 4.1	—
$FeCl_3$	31.4 ± 1.1	10.9 ± 0.3

BoXyl43A had 88, 88, 81 and 94% identical residues to those of RS233BX, RUM630-BX, CoXyl and BoXA.

Further, it was found that the amino acid sequence of BoXA had 81% identity to RS233BX. However, they exhibited different activity toward divalent metal. BoXyl43A and RS233BX exhibit same response to divalent metal ions. Although BoXyl43A and BoXA belong to the same family and display over 70% identity of amino acid sequences, they exhibit different responses to divalent metal ions. BoXyl43A was activated by divalent metal, while BoXA was not. Comparing the amino acid sequences in the active-site pocket between BoXyl43A and BoXA, it was found that the R110 in active-site pocket of BoXA was replaced by H110 of BoXyl43A. The differences of amino acids in the active-sites pockets might result in differences of BoXyl43A and BoXA which were both from *B. ovatus*.

Table 3. Relative activity of BoXyl43A on different substrates.

Substrate	Relative activity (%)[a]
*p*NPαAra*f*	51.3 ± 2.3
*p*NPαAra*p*	4.70 ± 0.3
*p*NPβXyl	100
*p*NPαGal	—
*p*NPβGal	29.2 ± 2.2
*p*NPαGlc	—
*p*NPβGlc	13.1 ± 1.6

[a]The activity of BoXyl43A on *p*NPβXyl was defined as 100%.

Substrate specificity of recombinant BoXyl43A

Activity of BoXyl43A was examined by using aryl-glycosides. The results showed that BoXyl43A exhibited activity towards *p*NPβXyl and *p*NPαAra*f*. In addition, it also had little activity on *p*NPαGal, *p*NPβGlc and *p*NPαAra*p* (Table 3). The results indicated that BoXyl43A from the GH43 family is a multifunctional β-xylosidase/α-L-arabinofuranosidase. The kinetic values K_m, V_{max}, and k_{cat} for *p*NPβXyl at 25 °C and pH 7.0 were 1.71 ± 0.21 mM, 7.41 ± 0.81 μmol/min/mg and 4.58 ± 0.49 s^{-1}, respectively. The k_{cat}/K_m (catalytic efficiency) was calculated to be 2.68 ± 0.08 $s^{-1}mM^{-1}$.

In order to analyze the selectivity of BoXyl43A to different substrates, carbohydrates mainly composed of arabinose or xylose were chosen to be hydrolyzed and released sugar could be detected by DNS Colorimetry. The results showed that BoXyl43A could hydrolyze xylooligosaccharide to release 126 ± 4 μg/mg of reducing sugar in 1 h and 141 ± 4 μg/mg in 12 h. However, when incubated with sugar beet arabinan or linear-1,5-α-L-arabinan for 12 h, BoXyl43A released negligible amounts of reducing sugars.

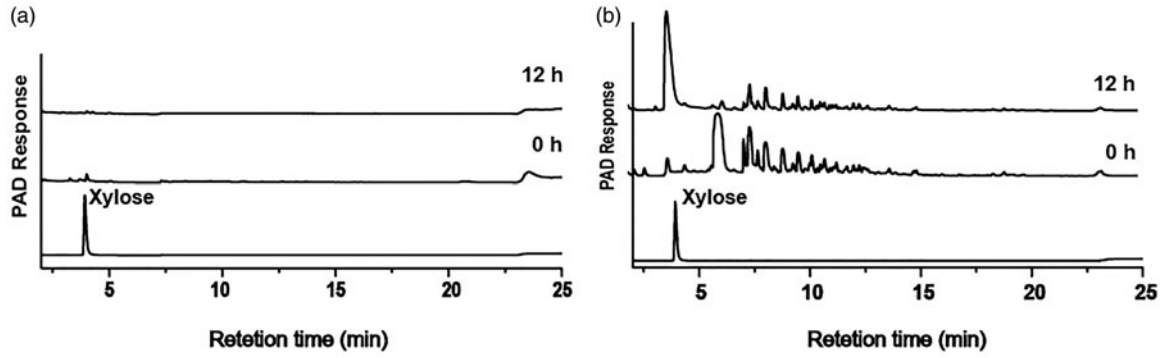

Figure 4. HPAEC analysis results of degradation products of wheat arabinoxylan (a) and xylooligosaccharide (b) by BoXyl43A. The substrates were incubated with BoXyl43A at 37 °C for 12 h.

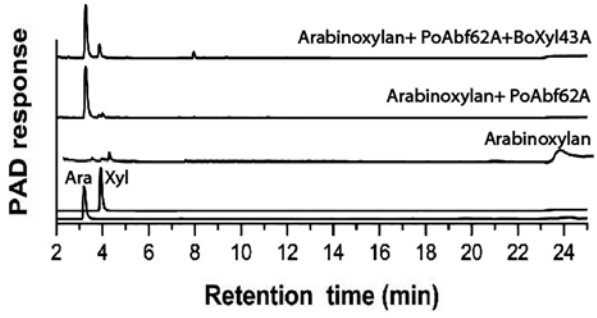

Figure 5. HPAEC analysis of the hydrolyzed products of arabinoxylan by the combination of recombinant BoXyl43A and PoAbf62A (α-L-arabinofuranosidase).

To verify the products of wheat arabinoxylan and xylooligosaccharide hydrolyzed by BoXyl43A, we monitored the release of monosaccharide or oligosaccharide using HPAEC. As shown in Figure 4, BoXyl43A could hydrolyze xylooligosaccharide and release xylose (Figure 4(b)), whereas it did not work on wheat arabinoxylan (Figure 4(a)). Therefore, we concluded that BoXyl43A was an exo-β-1,4-xylosidase.

Synergistic reaction of BoXyl43A and α-L-arabinofuranosidase in the degradation of arabinoxylan

Arabinoxylan consists of β-1,4-D-xylan as main chains and arabinose side chains. The side chains are linked to O-2/O-3 sites of xylan (Kormelink et al. 1993). Our experimental results showed that BoXyl43A could not hydrolyze arabinoxylan to release xylose. This might be caused by the arabinose in branches which prohibited BoXyl43A from degrading β-1,4-D-xylan. To verify this assumption, PoAbf62A cloned from *Pencillium oxalicum*, an α-L-arabinofuranosidase reported in our previous work, was used with BoXyl43A together to degrade arabinoxylan. It was known that PoAbf62A could specifically hydrolyze the arabinose in branches of arabinoxylan (Hu et al. 2018). Utilizing this property of PoAbf62A, we used it to successfully remove the arabinose side chains of arabinoxylan and release arabinose after 12 h of the reaction system at 37 °C and pH 4.5 (Figure 5). Next, we adjusted pH of reaction system to 7.0 and added BoXyl43A to the reaction system. The reaction was performed for 12 hours at 37 °C and xylose was released (Figure 5). Based on these results we could conclude that combination of BoXyl43A and PoAbf62A could degrade arabinoxylan and produce arabinose and xylose simultaneously.

Conclusion

BoXyl43A identified from the *B. ovatus* strain ATCC 8483 was overexpressed and characterized. BoXyl43A showed stability at pH 7.0 and temperature 35 °C. It exhibited an exo-type mode of action towards xylooligosaccharide and showed synergistic effect with α-L-arabinofuranosidase on degradation of arabinoxylan. BoXyl43A would have potential for application in hemicellulose degradation.

Disclosure statement

The authors report no conflict of interest. The authors alone are responsible for the content and writing of the paper.

Funding

This work was supported by the Key Scientific Program of Changchun City (No. 16CX20).

References

Carvalho DR, Carli S, Meleiro LP, Rosa JC, Arthur Oliveira HC, Jorge JA, Furriel R. 2018. A halotolerant bifunctional β-xylosidase/α-L-arabinofuranosidase from *Colletotrichum graminicola*: purification and biochemical characterization. Int J Biol Macromol. 114:741–750.

Cintra LC, Fernandes AG, Oliveira ICM, Siqueira SJL, Costa IGO, Colussi F, Jesuíno RSA, Ulhoa CJ, Faria FP. 2017. Characterization of a recombinant xylose tolerant β-xylosidase from *Humicola grisea* var. thermoidea and its use in sugarcane bagasse hydrolysis. Int J Biol Macromol. 105: 262–271.

Cragg SM, Beckham GT, Bruce NC, Bugg TD, Distel DL, Dupree P, Etxabe AG, Goodell BS, Jellison J, McGeehan JE, et al. 2015. Lignocellulose degradation mechanisms across the Tree of Life. Curr Opin Chem Biol. 29:108–119.

Gírio FM, Fonseca C, Carvalheiro F, Duarte LC, Marques S, Bogel-Łukasik R. 2010. Hemicelluloses for fuel ethanol: a review. Bioresour Technol. 101:4775–4800.

Hu YB, Yan XC, Zhang H, Liu JQ, Luo F, Cui YY, Wang WW, Zhou YF. 2018. Cloning and expression of a novel α-1,3-arabinofuranosidase from *Penicillium oxalicum* sp. 68. AMB Express. 8:51.

Isikgor FH, Becer CR. 2015. Lignocellulosic biomass: a sustainable platform for the production of bio-based chemicals and polymers. Polym Chem. 6:4497–4559.

Jordan DB, Braker JD, Wagschal K, Lee CC, Chan VJ, Dubrovska I, Anderson S, Wawrzak Z. 2015. X-ray crystal structure of divalent metal-activated β-xylosidase, RS223BX. Appl Biochem Biotechnol. 177:637–648.

Jordan DB, Braker JD, Wagschal K, Stoller JR, Lee CC. 2016. Isolation and divalent-metal activation of a β-xylosidase, RUM630-BX. Enzyme Microb Technol. 82:158–163.

Jordan DB, Stoller JR, Lee CC, Chan VJ, Wagschal K. 2017. Biochemical characterization of a GH43 β-xylosidase from *Bacteroides ovatus*. Appl Biochem Biotechnol. 182: 250–260.

Jordan DB, Wagschal K, Grigorescu AA, Braker JD. 2013. Highly active β-xylosidases of glycoside hydrolase family 43 operating on natural and artificial substrates. Appl Microbiol Biotechnol. 97:4415–4428.

Juturu V, Wu JC. 2012. Microbial xylanases: engineering, production and industrial applications. Biotechnol Adv. 30: 1219–1227.

Khandeparker R, Numan MT. 2008. Bifunctional xylanases and their potential use in biotechnology. J Ind Microbiol Biotechnol. 35:635–644.

Kim YA, Yoon KH. 2010. Characterization of a *Paenibacillus woosongensis* beta-xylosidase/alpha-arabinofuranosidase produced by recombinant *Escherichia coli*. J Microbiol Biotechnol. 20:1711–1716.

Knob A, Terrasa CRF, Carmona EC. 2010. β-Xylosidases from filamentous fungi: an overview. World J Microbiol Biotechnol. 26:389–407.

Kormelink FJM, Gruppen H, Voragen AGJ. 1993. Mode of action of (1-4)-beta-D-arabinoxylan arabinofuranohydrolase (AXH) and α-L-arabinofuranosidases on alkali-extractable wheat-flour arabinoxylan. Carbohydr Res. 249: 345–353.

Lagaert S, Pollet A, Courtin CM, Volckaert G. 2014. β-Xylosidases and α-l-arabinofuranosidases: accessory enzymes for arabinoxylan degradation. Biotechnol Adv. 32:316–332.

Lee CC, Braker JD, Grigorescu AA, Wagschal K, Jordan DB. 2013. Divalent metal activation of a GH43 β-xylosidase. Enzyme Microb Tech. 52:84–90.

Martens EC, Lowe EC, Chiang H, Pudlo NA, Wu M, McNulty NP, Abbott DW, Henrissat B, Gilbert HJ, Bolam DN, et al. 2011. Recognition and degradation of plant cell wall polysaccharides by two human gut symbionts. PLoS Biol. 9: e1001221.

Matsuzawa T, Kaneko S, Kishine N, Fujimoto Z, Yaoi K. 2017. Crystal structure of metagenomic β-xylosidase/ α-l-arabinofuranosidase activated by calcium. J Biochem. 162: 173–181.

Mendis M, Simsek S. 2015. Production of structurally diverse wheat arabinoxylan hydrolyzates using combinations of xylanase and arabinofuranosidase. Carbohydr Polym. 132: 452–459.

Saha BC. 2003. Hemicellulose bioconversion. J Ind Microbiol Biotechnol. 30:279–291.

Scheller HV, Ulvskov P. 2010. Hemicelluloses. Annu Rev Plant Biol. 61:263–289.

Somogyi M. 1952. Notes on sugar determination. J Biol Chem. 195:19–23.

Zhang M, Chekan JR, Dodd D, Hong PY, Radlinski L, Revindran V, Nair SK, Mackie RI, Cann I. 2014. Xylan utilization in human gut commensal bacteria is orchestrated by unique modular organization of polysaccharide-degrading enzymes. Proc Natl Acad. 111:3708–3717.